Applied Physics Letters

Interface conductance modal analysis of lattice matched InGaAs/InP

Cite as: Appl. Phys. Lett. **108**, 181606 (2016); https://doi.org/10.1063/1.4948520
Submitted: 26 January 2016 . Accepted: 21 April 2016 . Published Online: 05 May 2016

Kiarash Gordiz, and Asegun Henry

Interface conductance modal analysis of lattice matched InGaAs/InP

Kiarash Gordiz[1] and Asegun Henry[1,2,a)]
[1]*George W. Woodruff School of Mechanical Engineering, Georgia Institute of Technology, Atlanta, Georgia 30332, USA*
[2]*School of Materials Science and Engineering, Georgia Institute of Technology, Atlanta, Georgia 30332, USA*

(Received 26 January 2016; accepted 21 April 2016; published online 5 May 2016)

We studied the heat conduction at InGaAs/InP interfaces and found that the total value of interface conductance was quite high ~830 MW m^{-2} K^{-1}. The modal contributions to the thermal interface conductance (TIC) were then investigated to determine the mode responsible. Using the recently developed interface conductance modal analysis method, we showed that more than 70% of the TIC arises from extended modes in the system. The lattice dynamics calculations across the interface revealed that, unlike any other interfaces previously studied, the different classes of vibration around the interface of InGaAs/InP naturally segregate into distinct regions with respect to frequency. In addition, interestingly, the entire region of frequency overlap between the sides of the interface is occupied by extended modes, whereby the two materials vibrate together with a single frequency. We also mapped the correlations between modes, which showed that the contribution by extended modes to the TIC primarily arises from coupling to the modes that have the same frequencies of vibration (i.e., autocorrelations). Moreover, interfacial modes despite their low population still contribute more than 6% to interfacial thermal transport. The analysis sheds light on the nature of heat conduction by different classes of vibration that exist in interfacial systems, which has technological relevance to applications such as thermophotovoltaics and optoelectronics. *Published by AIP Publishing*. [http://dx.doi.org/10.1063/1.4948520]

Indium-gallium-arsenide alloys ($In_xGa_{1-x}As$) are of significant interest for thermophotovoltaics (TPV)[1,2] and other electronic systems.[3,4] In many instances, there is specific interest in the $In_{0.53}Ga_{0.47}As$ alloy, because it is lattice matched with InP,[5] which is commercially available as a single crystal substrate. This lattice matching makes this system an ideal platform for growing high quality single crystal devices, since there is minimal strain to drive the formation of defects, which can negatively affect the device performance.[6] Furthermore, since $In_{0.53}Ga_{0.47}As$ has an electronic band gap of 0.74 eV, it is an ideal candidate for TPV, since this band gap is close to the peak in the Black body spectrum at temperatures commensurate with many high temperature heat sources. In many applications, the devices consist of many successive layers with thicknesses ranging from as low as 10 nm up to 10 μm, and the temperature of the devices can often have a major influence on the performance. These devices therefore have to consider thermal management issues and one important quantity can be the thermal interface conductance (TIC) between the two materials.

Depending upon the device, low values of TIC could be highly important, if it presents a significant resistance to heat flow out of the system. However, many previous methods for studying TIC exhibit large discrepancies with experiments,[7–10] largely due to incomplete descriptions of the physics. In this respect, anharmonicity has proven to be one of the most important effects to include in TIC calculations.[11–15] Recently, Gordiz and Henry developed a new molecular dynamics (MD) based formalism termed the interface conductance modal analysis (ICMA) method that successfully incorporates anharmonicity.[16]

The ICMA method provides a new perspective on thermal transport through interfaces, because it is not derived using the phonon gas model (PGM), for which all other prior work on interfaces has been based.[13,15,17–20] Instead, the ICMA method is based on the following expression for TIC that was derived from the fluctuation-dissipation theorem[21] by Barrat *et al.*[22] and Domingues *et al.*[23]

$$G = \frac{1}{Ak_BT^2}\int_0^\infty \langle Q(t)Q(0)\rangle dt, \tag{1}$$

where G is the TIC between materials A and B, A is the cross-sectional contact area, k_B is the Boltzmann constant, T is the equilibrium system temperature, $\langle\cdots\rangle$ indicates calculation of the autocorrelation function, and Q represents the energy exchanged between materials A and B at each instant of time. The expression for Q can be written as

$$Q = -\sum_{i\in A}\sum_{j\in B}\left\{\frac{\mathbf{p}_i}{m_i}\cdot\left(\frac{-\partial H_j}{\partial \mathbf{r}_i}\right)+\frac{\mathbf{p}_j}{m_j}\cdot\left(\frac{\partial H_i}{\partial \mathbf{r}_j}\right)\right\}, \tag{2}$$

where i and j are the indices for the atoms in the system, the position and momentum of the atoms in the system are denoted by $\mathbf{r}_i$ and $\mathbf{p}_i$, respectively, and H_i represents the individual atom Hamiltonian which can be written as

$$H_i = \frac{\mathbf{p}_i^2}{2m_i} + \Phi_i(\mathbf{r}_1, \mathbf{r}_2, \ldots, \mathbf{r}_n), \tag{3}$$

where Φ_i is the potential energy assigned to a single atom,[24,25] and m_i is the mass of atom i. The expression for

a)Author to whom correspondence should be addressed. Electronic mail: ase@gatech.edu

TIC in Eq. (1) describes the transport in terms of the degree of correlation in heat flow across the interface, which can be computed from a MD simulation. The key contribution of Gordiz and Henry, however, was the projection of the interfacial heat flux onto the individual modes of the system.[16] This can be done by first calculating the normal mode coordinate of velocity for mode n ($\dot{X}_n$) as,[26]

$$\dot{X}_n = \sum_i \frac{m_i^{1/2}}{N^{1/2}} \dot{\mathbf{x}}_i \cdot \mathbf{e}_{n,i}^*, \tag{4}$$

where $\dot{\mathbf{x}}_i$ is the velocity of atom i, N is the total number of atoms, $*$ represents complex conjugate, and $\mathbf{e}_{n,i}$ is the eigen vector for mode n assigning the direction and displacement magnitude of atom i. From the inverse of the operations in Eq. (4), we can describe the velocity of atom i as the summation of individual contributions by different modes of vibration in the system as

$$\dot{\mathbf{x}}_i = \sum_n \frac{1}{(Nm_i)^{1/2}} \mathbf{e}_{n,i} \dot{X}_n. \tag{5}$$

Then, replacing Eq. (5) in the definition for interfacial heat flux (Eq. (2)) results in the following definition which is the contribution by mode of vibration n to the total interfacial heat flux

$$Q_n = \frac{1}{N^{1/2}} \sum_{i\in A} \sum_{j\in B} \left\{ \left(\frac{1}{(m_i)^{1/2}} \mathbf{e}_{n,i} \dot{X}_n \right) \cdot \left(\frac{\partial H_j}{\partial \mathbf{r}_i} \right) + \left(\frac{1}{(m_j)^{1/2}} \mathbf{e}_{n,j} \dot{X}_n \right) \cdot \left(\frac{-\partial H_i}{\partial \mathbf{r}_j} \right) \right\}, \tag{6}$$

where $Q = \sum_n Q_n$. Incorporating the above expression for Q_n in the definition of total conductance (Eq. (1)) yields the following definition for the individual modal contributions to TIC

$$G_n = \frac{1}{Ak_BT^2} \int \langle Q_n(t) Q(0) \rangle dt, \tag{7}$$

where $G = \sum_n G_n$. Replacing for both of the total heat fluxes in Eq. (1) using the modal heat flux definition in Eq. (6) also allows the calculation of the individual contributions from pairs of modes of vibration equal to

$$G_{n,n'} = \frac{1}{Ak_BT^2} \int \langle Q_n(t) Q_{n'}(0) \rangle dt. \tag{8}$$

The above equation provides a quantitative description for the degree of correlation between different pairs of modes in the system, which is in qualitative agreement with the concepts of diagonal and collective contributions introduced by Gill-Comeau and Lewis.[27,28]

Another important realization by Gordiz and Henry was the recognition that one cannot use the modes associated with the bulk materials to properly describe the interfacial heat flow.[29] Moreover, in the process of developing ICMA, Gordiz and Henry have shown that, based on the degree of localization of vibrational energy near the interface, the modes of vibration can be classified into four groups of modes, namely, ⟨1⟩ extended modes, ⟨2⟩ partially extended modes, ⟨3⟩ isolated modes, and ⟨4⟩ interfacial modes.[29] Observation of these types of modes can be attributed to the interface itself, whereby it breaks the system's symmetry and changes the dynamical matrix in such a way that localization occurs. Therefore, not all solutions for this modified dynamical matrix are capable of retaining the sinusoidally modulated eigen vectors for all of the atoms. Extended modes are delocalized over the entire system (Fig. 2(a)). Partially extended modes have vibrations on one side of the interface; however, the vibrations only partially extend through the interface and to the other side (Figs. 2(b) and 2(c)). Isolated modes exist only on one side of the interface and do not include participation near the interface (Fig. 2(d)). Interfacial modes are localized/peaked near the interface and majorly incorporate interfacial atoms into their vibrations (Fig. 2(e)). The nature of these modes' contributions to the TIC can be fundamentally different, as Gordiz and Henry[30] have also recently shown that interfacial modes can exhibit extremely large contributions and can serve as a bridge between the two materials, by coupling to many other modes. Thus, one of the key benefits of using ICMA is that it can describe any of the modes that exist in an interfacial structure, which can have a different character and associated roles in the heat conduction process. The PGM based descriptions, however, assume that all modes are propagating modes, which have a well-defined velocity.[31] Thus the PGM perspective is unable to account for the effect that an interface has on the mode character in a given structure. Therefore, in this study, we used the ICMA method to not only quantify but also understand the various contributions to TIC from different phonons in the $In_{0.53}Ga_{0.47}As$/InP system.

We used ICMA and equilibrium MD to calculate the modal contributions to TIC. The interactions are described by Tersoff interatomic potential[32] based on the parameters by Powell *et al.*[33] to model different III-V semiconductor compounds, and we used mixing rules[32] to describe the cross species interactions. Periodic boundary conditions have been applied to all three Cartesian coordinates, and a time step of 0.5 fs is chosen for the MD simulations. The number of unit cells along the xyz directions has been chosen to be equal to 3, 3, and 24 ($3 \times 3 \times 24$). We examined the effect of larger cross sections up to 5–5 unit cells and longer systems up to 50 unit cells, and neither resulted in changes larger than 5% to both the mode distributions from lattice dynamics (LD) or modal contributions to TIC calculated from MD. The interface is situated normal to the z direction, which is parallel to the [100] crystallographic direction, and the simulation temperature was set equal to 300 K. After relaxing the structure under the isobaric-isothermal ensemble (NPT) for 1 ns at zero pressure and $T = 300$ K and under the canonical ensemble (NVT) for another 1 ns at $T = 300$ K, we simulated the structure in the microcanonical (NVE) ensemble for 10 ns during which the modal contributions to the heat flux across the interface are calculated. The heat flux contributions are saved and post processed to calculate the mode-mode heat flux correlation functions.[16] The effect of different configurations on the InGaAs side has been accounted for by

averaging the results over five different random alloy configurations. Statistical uncertainty, due to insufficient phase space averaging, has been reduced to less than 5% by considering 10 independent ensembles.[34] The MD simulations were performed using the Large Atomic/Molecular Massively Parallel Simulator (LAMMPS),[35] and the LD calculations were performed using the General Utility Lattice Program (GULP).[36] The low-temperature LD information used in this study is justified because the simulation temperature of 300 K is lower than the temperatures (e.g., 800 K) at which Feng *et al.*[37] and Gill-Comeau and Lewis[27] have reported noticeable changes in frequencies and eigen vectors for their modal analysis. This effect is also not expected to dramatically change the results for this system.

Similar to previous studies, we observed four different types of modes arising from the LD of the entire structure of InGaAs/InP interface. Interestingly, unlike previous systems,[29,30] these modes are actually segregated into well-defined regions based on their frequencies. Figure 1(b) shows the total density of states (DOS) and DOS for each type of vibration at the interface of InGaAs/InP. In addition, the eigen vectors of vibration for a sample eigen mode of vibration belonging to each class of vibration are provided in Fig. 2. The segregation of the modes according to their frequencies is different from previous observations of Ar based interfaces,[29,38] Si interfaces with mass difference,[29] or Si/Ge interfaces[30] in which different types of vibrational modes appear in overlapping regions of the DOS. It is also peculiar that even the partially extended modes on InP side and partially extended modes on InGaAs side occupy separate sections on DOS. The primary cause of the mode segregation is the phonon band gap in InP. InP has a large gap in its vibrations between ~5.9 and 10 THz (see Fig. 1(a)), largely due to the significant mass difference in the basis (~3.5×). The lack of vibrational states between 5.9 and 10 THz in InP forces the system to segregate the modes of the full structure into distinct regimes.

From Fig. 1(a), it can be seen that the interfacial modes exist at two narrow bands of frequencies: (1) the point where extended modes transition into partially extended modes on InGaAs side, and (2) the onset of partially extended modes

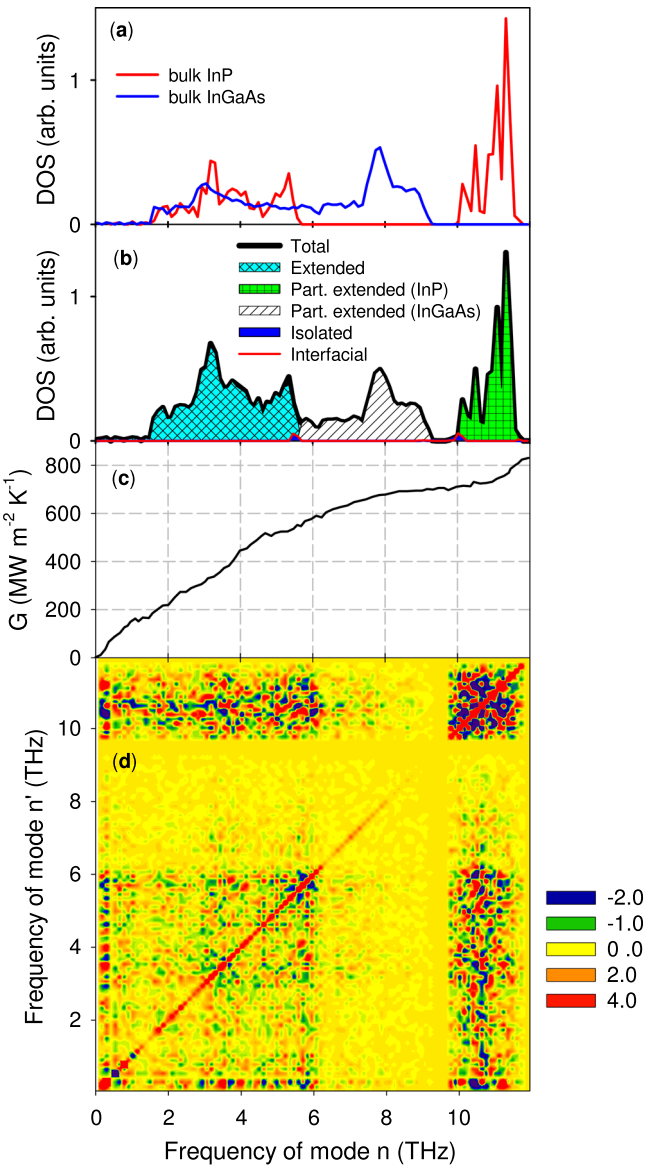

FIG. 1. DOS and modal contributions to TIC for InGaAs/InP interface at T = 300 K. (a) DOS for isolated InP and isolated InGaAs before making interface, (b) total DOS and DOS for different mode classifications across the interface, (c) TIC accumulation function, and (d) 2D map showing the magnitudes of the correlations/interactions on the plane of two frequency axes. The values presented on the 2D map have units of MW m^{-2} K^{-1}.

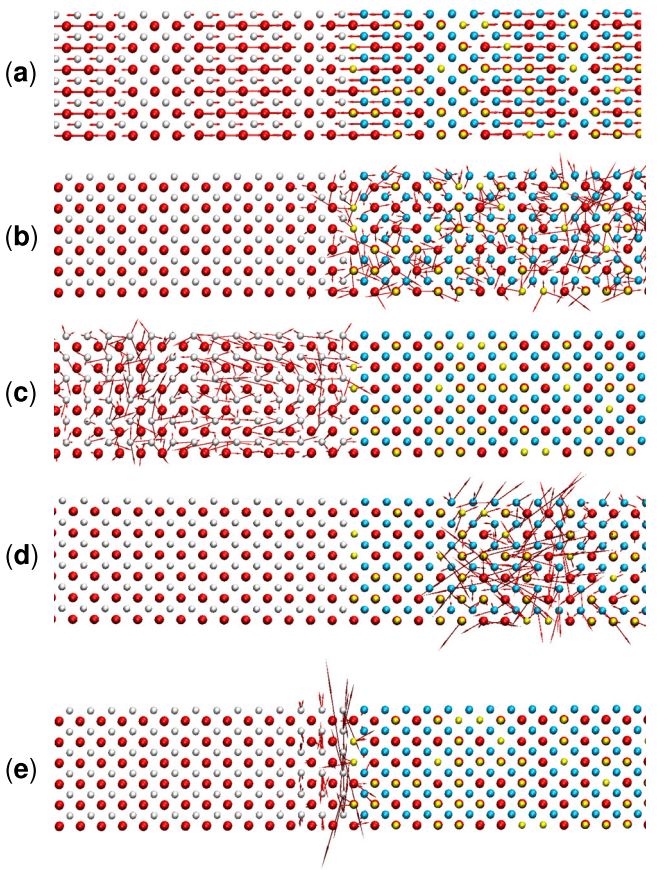

FIG. 2. Eigen vectors for different examples of the four classes of vibration present at the interface of InGaAs/InP. In, Ga, As, and P atoms are represented by red, yellow, cyan, and white spheres, respectively. The examples and their frequencies are (a) extended mode at 3.86 THz, (b) partially extended mode centered on InGaAs side at 8.11 THz, (c) partially extended mode centered on InP side at 10.61 THz, (d) isolated mode at 5.48 THz, and (e) interfacial mode at 9.96 THz.

TABLE I. Number of states for the four different classes of vibration and their contribution to TIC across the InGaAs/InP interface. Columns 2–4 represent the fraction of the total number of states ($\overline{DOS}$), the percentage contribution to G ($\bar{G}$), and contribution to G divided by fraction of total number of states (i.e., contribution to G per mode) ($\bar{G}/\overline{DOS}$), respectively.

Mode type	$\overline{DOS}(\%)$	$\bar{G}(\%)$	$\bar{G}/\overline{DOS}$
Extended	47.1	70.6	1.50
Partially extended	52.6	23.1	0.44
Isolated	0.1	<0.01	<0.01
Interfacial	0.2	6.3	31.5

on InP side. Also, interestingly Table I shows that, by comparison to previously studied structures, the $In_{0.53}Ga_{0.47}As$/InP structure has significantly more extended modes ~47%, which is larger than a previously studied Ar/4Ar interface ~10% (Ref. 29) and Si/Ge interface ~30%.[30] In essence, since extended modes correspond to collective vibrations of the entire system (e.g., including both bulk materials together) at a single frequency, their fraction of the total number of states is commensurate with the bulk DOS overlap. However, Gordiz and Henry showed that, for instance, at the interface of Ar(m)/Ar(4 m), a large population of partially extended modes exist even at the region of frequency overlap between the two sides of the interface.[29] This observation showed that DoS overlap does not automatically guarantee that the states will be extended. Nonetheless, for the $In_{0.53}Ga_{0.47}As$/InP structure, interestingly all of the eigen modes in the regions of DoS overlap fall into class $\langle 1 \rangle$ and are extended. Thus, the $In_{0.53}Ga_{0.47}As$/InP structure appears to have the maximum number of extended modes possible.

After calculating the modal contributions to TIC, it was found that interfacial modes have the highest per mode contribution (see Table I), similar to Ar/4Ar[29] and Si/Ge interfaces.[30] Fig. 1(c) shows that the conductance accumulation associated with the low frequency modes (e.g., between 0 and 1 THz) is large, ~20% of the total TIC. The large value observed for the total TIC also suggests that in InGaAs/InP devices, this particular interface likely contributes negligible resistance to the overall device resistance.

Using ICMA, the degree of interaction/correlation between each pair of vibrational modes in the system can be calculated and presented as a two-dimensional map of correlation,[16,29] shown in Fig. 1(d). Since elastic interactions are restricted to phonons of the same frequency, which are only associated with the values along the diagonal of the correlation map (Fig. 1(d)), all the off-diagonal contributions are attributed to the anharmonicity. It is interesting to note that the large contribution by extended modes (~70%) including the contribution by low frequency modes between 0 and 1 THz mainly arises from the auto-correlations, while for partially extended modes, particularly the ones that are located on the InP side, the major contributions to TIC are caused by cross-correlations. In fact, since the frequency of vibration for the partially extended modes on InP side is larger than the maximum frequency of vibration on InGaAs side, the contribution by these modes is attributed to anharmonicity. Particularly, it can be seen from 2D correlation map that partially extended modes on InP side are primarily correlated with lower frequency extended modes in the system. Moreover, not only because of their considerable contribution to conductance (~12%), but also because of their strong band of anharmonic coupling, the contributions by partially extended modes on the InP side, to a great degree, resemble the contributions by interfacial modes in crystalline Si/Ge interfaces.[30] In addition, the degree of cross-correlations for partially extended modes primarily located on InP side seem much stronger compared to the cross-correlations for partially extended modes primarily located in InGaAs. It can also be seen from Fig. 1(d) that the frequency-doubling and frequency-halving processes that was reported to be significant for Ar(m)/Ar(4 m) interface[15] do not seem to be the dominant correlations for the interface of InP/InGaAs.

These observations lead to the following interpretations. (1) The extended modes behave almost as their own subsystem and exhibit minimal interaction with other modes in the system. Since they extend through the entire structure, it is as if they do not recognize the presence of the interface and thus, their contributions may not be well explained by a picture framed upon the PGM, e.g., it is as if they simply contribute directly to the total thermal conductivity of the full structure based on their respective mean free paths. (2) The fact that the partially extended mode contributions are dominated by their cross-correlations suggests that these mode's contributions may be well described by the PGM transmission paradigm. This is because cross-correlation is a signal of interaction, and therefore, these modes, which on the InP side are essentially propagating modes, carry energy to the interface and then exchange it with other modes on the other side via scattering. (3) The fact that the high frequency modes, above the phonon band gap in InP, contribute primarily via cross correlation is consistent with the conventional PGM model, since there are no modes on with the same frequencies on the other side that they can exchange energy with. Therefore, all of their contributions can be associated with inelastic interactions/anharmonic effects. Furthermore, the fact that their contributions are non-negligible ~12% suggests that, again, as was observed for other systems[11–15] anharmonicity is non-negligible at room temperature.

In conclusion, we studied the InGaAs/InP interface and found an interesting result, whereby remarkably the normal modes of vibration segregate into distinct regions of frequency. Second, the TIC is very high and is not likely to be limiting in devices with layer thicknesses greater than ~15 nm. The majority of the TIC comes from the extended modes and various correlations for each group of modes indicates that the extended modes behave as if the interface is non-existent, while the partially extended modes behave in a manner more consistent with the conventional paradigm based on the PGM. This application of the ICMA method provides insight and useful data for future studies focused on thermal management in systems containing InGaAs/InP interfaces, as there is now evidence to suggest that the TIC is large and may be negligible by comparison to the thermal resistance of the respective device layers.

[1]G. Charache, J. Egley, D. Depoy, L. Danielson, M. Freeman, R. Dziendziel, J. Moynihan, P. Baldasaro, B. Campbell, and C. Wang, "Infrared materials for thermophotovoltaic applications," J. Electron. Mater. **27**, 1038–1042 (1998).

[2]T. J. Coutts, "An overview of thermophotovoltaic generation of electricity," Sol. Energy Mater. Sol. Cells **66**, 443–452 (2001).
[3]A. Tosi, A. Della Frera, A. B. Shehata, and C. Scarcella, "Fully programmable single-photon detection module for InGaAs/InP single-photon avalanche diodes with clean and sub-nanosecond gating transitions," Rev. Sci. Instrum. **83**, 013104 (2012).
[4]H. Ito, T. Furuta, S. Kodama, and T. Ishibashi, "InP/InGaAs uni-travelling-carrier photodiode with 310 GHz bandwidth," Electron. Lett. **36**, 1809–1810 (2000).
[5]S. Forrest, O. Kim, and R. Smith, "Optical response time of $In_{0.53}Ga_{0.47}As$/InP avalanche photodiodes," Appl. Phys. Lett. **41**, 95–98 (1982).
[6]J. Cederberg, J. Blaich, G. Girard, S. Lee, D. Nelson, and C. Murray, "The development of (InGa) As thermophotovoltaic cells on InP using strain-relaxed In (PAs) buffers," J. Cryst. Growth **310**, 3453–3458 (2008).
[7]R. M. Costescu, M. A. Wall, and D. G. Cahill, "Thermal conductance of epitaxial interfaces," Phys. Rev. B **67**, 054302 (2003).
[8]R. Stoner and H. Maris, "Kapitza conductance and heat flow between solids at temperatures from 50 to 300 K," Phys. Rev. B **48**, 16373 (1993).
[9]H.-K. Lyeo and D. G. Cahill, "Thermal conductance of interfaces between highly dissimilar materials," Phys. Rev. B **73**, 144301 (2006).
[10]P. E. Hopkins, J. C. Duda, S. P. Clark, C. P. Hains, T. J. Rotter, L. M. Phinney, and G. Balakrishnan, "Effect of dislocation density on thermal boundary conductance across GaSb/GaAs interfaces," Appl. Phys. Lett. **98**, 161913 (2011).
[11]P. E. Hopkins, P. M. Norris, and J. C. Duda, "Anharmonic phonon interactions at interfaces and contributions to thermal boundary conductance," J. Heat Transfer **133**, 062401 (2011).
[12]R. J. Stevens, L. V. Zhigilei, and P. M. Norris, "Effects of temperature and disorder on thermal boundary conductance at solid–solid interfaces: Nonequilibrium molecular dynamics simulations," Int. J. Heat Mass Transfer **50**, 3977–3989 (2007).
[13]Y. Chalopin and S. Volz, "A microscopic formulation of the phonon transmission at the nanoscale," Appl. Phys. Lett. **103**, 051602 (2013).
[14]Z.-Y. Ong and E. Pop, "Frequency and polarization dependence of thermal coupling between carbon nanotubes and SiO_2," J. Appl. Phys. **108**, 103502 (2010).
[15]K. Sääskilahti, J. Oksanen, J. Tulkki, and S. Volz, "Role of anharmonic phonon scattering in the spectrally decomposed thermal conductance at planar interfaces," Phys. Rev. B **90**, 134312 (2014).
[16]K. Gordiz and A. Henry, "A formalism for calculating the modal contributions to thermal interface conductance," New J. Phys. **17**, 103002 (2015).
[17]E. Swartz and R. Pohl, "Thermal resistance at interfaces," Appl. Phys. Lett. **51**, 2200–2202 (1987).
[18]N. Mingo and L. Yang, "Phonon transport in nanowires coated with an amorphous material: An atomistic Green's function approach," Phys. Rev. B **68**, 245406 (2003).
[19]P. K. Schelling, S. R. Phillpot, and P. Keblinski, "Phonon wave-packet dynamics at semiconductor interfaces by molecular-dynamics simulation," Appl. Phys. Lett. **80**, 2484–2486 (2002).
[20]I. M. Khalatnikov, "Teploobmen Mezhdu Tverdym Telom I Geliem-Ii," Z. Eksp. Teor. Fiz. **22**, 687–704 (1952).
[21]R. Kubo, "The fluctuation-dissipation theorem," Rep. Prog. Phys. **29**, 255 (1966).
[22]J.-L. Barrat and F. Chiaruttini, "Kapitza resistance at the liquid—solid interface," Mol. Phys. **101**, 1605–1610 (2003).
[23]G. Domingues, S. Volz, K. Joulain, and J.-J. Greffet, "Heat transfer between two nanoparticles through near field interaction," Phys. Rev. Lett. **94**, 085901 (2005).
[24]R. J. Hardy, "Energy-flux operator for a lattice," Phys. Rev. **132**, 168 (1963).
[25]A. S. Henry and G. Chen, "Spectral phonon transport properties of silicon based on molecular dynamics simulations and lattice dynamics," J. Comput. Theor. Nanosci. **5**, 141–152 (2008).
[26]M. T. Dove, *Introduction to Lattice Dynamics* (Cambridge University Press, 1993), Vol. 4.
[27]M. Gill-Comeau and L. J. Lewis, "Heat conductivity in graphene and related materials: A time-domain modal analysis," Phys. Rev. B **92**, 195404 (2015).
[28]M. Gill-Comeau and L. J. Lewis, "On the importance of collective excitations for thermal transport in graphene," Appl. Phys. Lett. **106**, 193104 (2015).
[29]K. Gordiz and A. Henry, "Phonon transport at interfaces: Determining the correct modes of vibration," J. Appl. Phys. **119**, 015101 (2016).
[30]K. Gordiz and A. Henry, "Phonon transport at crystalline Si/Ge interfaces: the role of interfacial modes of vibration," Sci. Rep. **6**, 23139 (2016).
[31]G. Chen, *Nanoscale Energy Transport and Conversion: A Parallel Treatment of Electrons, Molecules, Phonons, and Photons* (Oxford University Press, USA, 2005).
[32]J. Tersoff, "Modeling solid-state chemistry: Interatomic potentials for multicomponent systems," Phys. Rev. B **39**, 5566 (1989).
[33]D. Powell, M. Migliorato, and A. Cullis, "Optimized Tersoff potential parameters for tetrahedrally bonded III-V semiconductors," Phys. Rev. B **75**, 115202 (2007).
[34]K. Gordiz, D. J. Singh, and A. Henry, "Ensemble averaging vs. time averaging in molecular dynamics simulations of thermal conductivity," J. Appl. Phys. **117**, 045104 (2015).
[35]S. Plimpton, "Fast parallel algorithms for short-range molecular dynamics," J. Comput. Phys. **117**, 1–19 (1995).
[36]J. D. Gale, "GULP: A computer program for the symmetry-adapted simulation of solids," J. Chem. Soc., Faraday Trans. **93**, 629–637 (1997).
[37]T. Feng, B. Qiu, and X. Ruan, "Anharmonicity and necessity of phonon eigenvectors in the phonon normal mode analysis," J. Appl. Phys. **117**, 195102 (2015).
[38]K. Gordiz and A. Henry, "Examining the effects of stiffness and mass difference on the thermal interface conductance between Lennard-Jones solids," Sci. Rep. **5**, 18361 (2015).